Food and Chemical Toxicology 125 (2019) 605–613

Contents lists available at ScienceDirect

Food and Chemical Toxicology

journal homepage: www.elsevier.com/locate/foodchemtox

Identification of narciclasine from *Lycoris radiata* (L'Her.) Herb. and its inhibitory effect on LPS-induced inflammatory responses in macrophages

Chun-Yan Shen, Xi-Lin Xu*, Lin-Jiang Yang, Jian-Guo Jiang**

College of Food and Bioengineering, South China University of Technology, Guangzhou, 510640, China

ARTICLE INFO

Keywords:
Narciclasine
Anti-inflammation
Anti-Cancer
Lycoris radiata

ABSTRACT

Lycoris radiata (L'Her.) Herb. (*L. radiata*) was traditionally used as a folk medicine in China for treatment of Alzheimer's disease. However, the specific component responsible for its considerable toxicity remained unclear thus restricting its clinical trials. Narciclasine (NCS) was isolated from *L. radiata* and treatment of NCS for 72 h exhibited significant antiproliferative effects against L02, Hep G2, HT-29 and RAW264.7 cells. However, what needs to be emphasized is that at safe working concentrations of 0.001–0.016 μM, administration of NCS for 24 h inhibited the mRNA expression of inducible nitric oxide synthase (iNOS), interleukin-6 (IL-6), tumor necrosis factor-alpha (TNF-α), interleukin-1beta (IL-1β) and cyclooxygenase-2 (COX-2) in lipopolysaccharide (LPS)-induced macrophages thereby suppressing production of nitric oxide (NO), IL-6, TNF-α and IL-1β. NCS supplementation also inhibited nuclear factor-kappa B (NF-κB) activation by suppressing NF-κB P65 phosphorylation and nuclear translocation, IκBα degradation and phosphorylation, and IκKα/β phosphorylation. The phosphorylation of c-Jun N-terminal kinase (JNK) and P38, and expression of COX-2 was also attenuated by NCS. These results suggested that NCS might exert anti-inflammatory effects through inhibiting NF-κB and mitogen-activated protein kinase (MAPK) pathways even at very low doses.

1. Introduction

The mitogen-activated protein kinase (MAPK) and nuclear factor-kappa B (NF-κB) signaling pathways played important roles in regulating numerous of inflammation-associated genes, cytokines, enzymes and chemokines. NF-κB generally exists in a heterodimeric inactive form in the cytosol bound to distinct inhibitory IκB subunits. Nevertheless, IκBα degradation and phosphorylation could lead to NF-κB activation. The liberated NF-κB would translocate from the cytosol into the nuclei, thereby leading to the inflammation progression. Reportedly, MAPK might be an up-stream activator of NF-κB signaling pathway (Caivano, 1998; Vanden Berghe et al., 1998). Thus, MAPK and NF-κB were prominent targets for screening novel drugs with anti-inflammatory effects.

Lycoris radiata (L'Her.) Herb. (*L. radiata*), belonging to the Amaryllidaceae family and *Lycoris* genus, was traditionally used in China as a folk medicine. *L. radiata* was generally considered toxic, however, the specific component responsible for its toxicity was still unclear. The pharmacologically most interesting secondary metabolites present in plants of *L. radiata* were alkaloids. Among various types of alkaloids, Amaryllidaceae alkaloids were found to exert diverse pharmacological activities including anticancer/cytotoxic, anti-inflammatory, antibacterial, antiretroviral and antimalarial properties (He et al., 2015; Sener et al., 2003). For example, lycorine significantly inhibited inducible nitric oxide synthase (iNOS) and cyclooxygenase-2 (COX-2) expression in lipopolysaccharide (LPS)-induced RAW264.7 cells (Kang et al., 2012).

Specifically, the Amaryllidaceae isocarbostyril alkaloid narciclasine (NCS), also known as lycoricidinol was firstly discovered in *Narcissus* species in 1967. Then, it became a hotspot and was intensively investigated as an anticancer compound because of its significant and selective cytotoxic effects on cancer cells (Li et al., 2013; Pettit et al., 2001; Van Goietsenoven et al., 2010, 2013). The National Cancer Institute panel investigated the cytotoxic activity of NCS on 60 human tumor cell lines and the mean IC_{50} value were determined to be 0.046 μM. Recently, a new field of indication has emerged: a growing number of published data have justified that NCS could exert potent anti-inflammatory effects *in vivo* and *in vitro*. For example, Mikami et al. found that NCS showed effective prophylactic actions on the adjuvant arthritis model in rats (Mikami et al., 1999). Lubahn et al. further demonstrated that the sodium narcistatin, a water-soluble cyclic phosphate pro-drug of NCS, dramatically reduced inflammation (Lubahn

* Corresponding author. College of Food Science and Technology, South China University of Technology, Guangzhou, 510640, China.
** Corresponding author. College of Food Science and Technology, South China University of Technology, Guangzhou, 510640, China.
E-mail addresses: xuxilin@scut.edu.cn (X.-L. Xu), jgjiang@scut.edu.cn (J.-G. Jiang).

https://doi.org/10.1016/j.fct.2019.02.003
Received 6 November 2018; Received in revised form 29 January 2019; Accepted 1 February 2019
Available online 07 February 2019
0278-6915/

et al., 2012). The authors ascribed this to the inhibition of pro-inflammatory cytokines secretion by sodium narcistatin. Additionally, both Yui et al. and Yamazaki et al. reported that NCS showed tumor necrosis factor-alpha (TNF-α) suppressive effects in LPS-induced RAW264.7 cells (Yamazaki and Kawano, 2011; Yui et al., 2001). Nevertheless, the underlying molecular mechanism by which NCS exerted the anti-inflammatory effects still remained elusive.

In this paper, we strived to isolate and identify NCS on the basis of column chromatography and spectroscopic methods. Furthermore, we evaluated the cytotoxicity of NCS on human normal cell line of L02 (liver cell), human cancer cell line of HT-29 (colon carcinoma), Hep G2 (liver cancer), HeLa (cervix carcinoma), MCF-7 (breast cancer) and murine macrophage RAW264.7 using MTT method. Additionally, LPS-stimulated RAW264.7 cells were employed to investigate the anti-inflammatory effects of NCS in order to explore its underlying mechanism.

2. Material and methods

2.1. Plant materials

The whole aerial parts of *L. radiata* were purchased from Qingping TCM market (Guangzhou, China) and authenticated by the authors. A specimen (2015002) was deposited in South China University of Technology, Guangzhou, China. *L. radiata* were carefully ground in a cutting mill and then passed through a 50-mesh sieve to obtain fine powders. The powders were stored in sealing bags in the desiccators for future research.

2.2. Reagents

Dulbecco's modified Eagle's medium, fetal bovine serum and Trizol Reagent were purchased from GIBCO (Grand Island, NY). LPS weas purchased from Sigma-Aldrich (St. Louis, MO, USA). Silica gel 60 and sephadex LH-20 were obtained from Beijing H&E Ltd Corporation (Beijing, China). Mouse ELISA kits for interleukin-6 (IL-6), TNF-α and interleukin-1β (IL-1β) for immunohistochemistry were obtained from Cusabio Biotech CO., Ltd. (Wuhan, China). Nitric oxide assay kit, RIPA lysis buffer and nuclear and cytoplasmic protein extraction kit were purchased from Beyotime Biotech (Guangzhou, China). Antibodies for GAPDH, p-c-Jun N-terminal kinase (JNK), p-P38, nuclear factor-kappa B P65 (NF-κB P65), p-P65, IκBα, p-IκBα, p-IκKα/β, COX-2 and horseradish peroxidase-linked secondary antirabbit were obtained from Cell Signaling Technology (Beverly, MA). The dilution of antibodies and their catalog numbers were all provided in Table 1.

2.3. Extraction and isolation

The process of *L. radiata* extraction was demonstrated in supplementary material Fig. S1. Briefly, the dried aerial and bulbs of *L. radiata* (5 kg) were extracted at 100 °C by reflux with 75% ethanol for 3 h. Then the extracted solutions were centrifuged at 4000 rpm for 10 min, concentrated under reduced power and evaporated in the drying oven to give the brownish residues. Then, the brownish residues were suspended in methanol and partitioned successively with petroleum ether, ethyl acetate, n-butanol and water to yield the petroleum ether fraction (30.2 g), ethyl acetate fraction (49.8 g), n-butanol fraction (40.4 g) and water fraction (45.2 g). The ethyl acetate extracts (49.8 g) were concentrated under reduced power to yield the ethyl acetate layer of *L. radiata*. The ethyl acetate fractions were subjected to column chromatography over a silica gel column (80 × 1200 mm, 200–300 mesh) by elution with chloroform-methanol gradients (*v/v*) of 100:0, 100:5, 100:8, 100:10, 100:15, 100:18, 80:20, 70:30, 50:50 and 0:100. Every gradient was applied with 5 column volumes of chloroform-methanol solutions and each column volume was 4 L. As a result, 44 fractions including fractions 1–2, fractions 3–7, fractions 8–12, fractions 13–17, fractions 18–22, fractions 23–27, fractions 28–32, fractions 33–37, fractions 38–42 and fractions 43–44 were collected after eluted with chloroform/methanol (*v/v*) at 100:0, 100:5, 100:8, 100:10, 100:15, 100:18, 80:20, 70:30, 50:50 and 0:100, respectively. The 44 fractions were then combined according to the thin-layer chromatography analysis thus resulting in 4 fractions (Fractions 11–18, Fractions 24–32, Fractions 43–47 and Fractions 54–61). Then the 4 fractions were further purified by repeated chromatography of ODS column (eluted with methanol-water gradients of 30%, 60%, 80% and 90%, v/v) and sephadex LH-20 column (eluted with methanol-water solutions of 50%, v/v). Eventually, the pure product was collected after alcohol or acetic acid crystallization of the eluted fractions. HPLC analysis indicated that the purity of the product exceeded 98%. Then its structural identification was achieved using spectroscopic techniques of ^{1}H and ^{13}C nuclear magnetic resonance.

2.4. Cell culture

The human normal cell line of L02, HT-29, Hep G2, HeLa, MCF-7 and RAW264.7 were purchased from the cell bank of Shanghai of Chinese Academy of Sciences and maintained in a 37 °C humidified incubator containing 5% CO_2. RAW264.7 cells were stimulated with LPS (1 μg/mL) in the presence or absence of NCS (0.001–0.016 μM). In the current experiment, NCS was dissolved in dimethyl sulfoxide (DMSO) and the final concentration of DMSO was maintained at 0.1% (*v/v*). The cells in control groups were treated with 0.1% (*v/v*) of DMSO.

2.5. MTT assay for cell cytotoxicity

Cell cytotoxicity of NCS was determined using MTT method based on the reduction of the tetrazolium salt MTT into formazan crystals (Shen et al., 2017b). Briefly, different kinds of cells including L02, HT-29, Hep G2, HeLa, MCF-7 and RAW264.7, were seeded in 96-well plates at a density of 1×10^4 cells/well and cultured overnight. Then the cells were incubated with various concentrations of NCS (0.001–0.016 μM) for 24 h or 72 h. Subsequently, MTT solution (5 mg/mL) was added to each well to make a final concentration of 0.5 mg/mL and continuously incubated for another 4 h. The absorbance at 490 nm was detected using microplate reader and the cell viability was calculated based on the ratio of average optical density between control cells and NCS-treated cells.

Table 1
The dilution of antibodies and their catalog numbers.

Antibodies	Dilution	Catalog number	Antibodies	Dilution	Catalog number
GAPDH (14C10) Rabbit mAb	1:1000	2118S	α-Tubulin (11H10) Rabbit mAb	1:1000	2125S
SAPK/JNK Antibody	1:1000	9252S	Lamin B1 (D9V6H) Rabbit mAb	1:1000	13435S
Phospho-SAPK/JNK (Thr183/Tyr185) (81E11) Rabbit mAb	1:1000	4668S	IκBα (44D4) Rabbit mAb	1:1000	4812S
p38 MAPK (D13E1) XP® Rabbit mAb	1:1000	8690S	Phospho-IκBα (Ser32) (14D4) Rabbit mAb	1:1000	2859S
Phospho-p38 MAPK (Thr180/Tyr182) (12F8) Rabbit mAb	1:1000	4631S	Phospho-IKKα/β (Ser176/180) (16A6) Rabbit mAb	1:1000	2697S
NF-κB p65 (D14E12) XP® Rabbit mAb	1:1000	8242S	Cox2 (D5H5) XP® Rabbit mAb	1:1000	12282S
Phospho−NF−κB p65 (Ser536) (93H1) Rabbit mAb	1:1000	3033S			

2.6. Nitric oxide and cytokines assay

Nitric oxide (NO) production was indicated by the nitrite release in the culture media as described in our laboratory (Shen et al., 2017b). The supernatants of RAW264.7 cells were carefully collected after stimulated with LPS in the presence or absence of NCS (0.001–0.016 μM) for 24 h. Griess reagents (Beyotime Biotech, Guangzhou, China) were then mixed with the supernatants and reacted for 10 min in the dark place at room temperature. Finally, the nitrite concentration was measured spectrophotometrically at 550 nm using microplate reader. The standard curve was plotted against different concentrations of sodium nitrite according to the manufactures' instructions. At the same time, representative micrographs of the macrophages were obtained by invert microscopes in order to observe the morphology changes. Furthermore, the secretion of IL-6 in the culture media, as well as TNF-α and IL-1β, was also determined using ELISA kits purchased from Cusabio Biotech CO., Ltd. (Wuhan, China). Each experiment was carried out at least three times in duplicate.

2.7. RT-qPCR analysis

Total RNA of RAW264.7 cells was extracted from the test samples using Trizol reagents (Grand Island, NY) according to the manufacturer's instructions to yield highly pure RNA. RNA concentration and purity were determined by the Nano Drop spectrophotometer (Nano Drop Technologies, Wilmington, DE). Then 3 μg of total RNA in a total volume of 20 μL was reverse-transcribed into cDNA and then amplified using the DyNAmo Flash SYRB Green qPCR Kit and the cycle conditions were set according to the published report (Shen et al., 2017c) as follows: 50 °C for 2 min, 95 °C for 10 min, 40 cycles of 95 °C for 30 s, 60 °C for 30 s. The PCR primers were synthesized and purchased from Life Technology Inc. (Rockville, MD). The primer sequences of GAPDH, iNOS, IL-6, TNF-α, IL-1β and COX-2 were shown in supplementary material Table S2. The relative expression levels of the target genes against that of the GAPDH were calculated using $2^{-\Delta\Delta}$Ct method. To make the experiment reproducible, the RT-qPCR analysis strictly followed the MIQE guideline published by Bustin et al. (2009). The non-template controls were also conducted.

2.8. Immuno-staining for translocation of P65

Nuclear translocation of NF-κB P65 was evaluated according to the published literature (Bender et al., 2018; Hu et al., 2012). In brief, after treatment with NCS for 12 h, the culture media were removed and RAW264.7 cells washed twice with PBS. Then, cells were fixed with 4% paraformaldehyde, blocked with 5% bovine serum albumin, incubated with the primary rabbit anti−NF−κB P65 antibody and the secondary Cy3-labeled antibody. Thereafter, the cells were stained with DAPI for 5 min and observed using a laser scanning confocal microscope (Carl Zeiss LSM 710, Germany) subsequently.

2.9. Western blot analysis

SDS–polyacrylamide gel electrophoresis (SDS-PAGE) and western blotting were conducted according to the previous reports with minor modifications (Shen et al., 2017b). RAW264.7 cells were harvested and washed twice with cold PBS. Then, total proteins were extracted from RAW264.7 cells by lysis on ice for 40 min with RIPA lysis buffer (Beyotime Biotech, Guangzhou, China) supplemented with PMSF. Simultaneously, cytosolic and nuclear proteins were extracted using the Nuclear and Cytoplasmic Protein Extraction Kit (Beyotime Biotech, Guangzhou, China). Briefly, the cytosolic fraction of RAW264.7 cells was prepared by centrifugation at 12,000 g for 5 min after incubated with cytoplasmic protein extraction agent A and B. The remaining pellets were then mixed with nuclear protein extraction agent and exerted with drastic vortex, thus resulting in the nuclear fraction. Protein concentrations were detected using BCA kit to make equal protein amount loaded onto each lane of SDS–PAGE. 40 μg protein of 25 μL from each tested sample was carefully loaded onto each lane of 8% SDS–polyacrylamide gels by electrophoresis and then transferred to PVDF membranes by electroblotting. Thereafter, the PVDF membranes were successively incubated with blocking solution, primary antibodies and horseradish peroxidase-conjugated anti-rabbit IgG. Eventually, the immunoreactive bands were visualized using the ECL-Plus detection system. The relative density of p-JNK, p-P38, NF-κB P65, p-P65, IκBα, p-IκBα, p-IκKα/β and COX-2 was normalized with GAPDH.

2.10. Statistics

Experimental data were expressed as the mean ± standard deviation of at least 5 independent experiments. One-way analysis of variance followed by post hoc Tukey's test was employed for multiple comparisons. Statistical analysis was conducted using SPSS 20.0 software. $p < 0.05$ was considered to be statistically significant and $p < 0.01$ was considered to be statistically highly significant.

3. Results

3.1. Structure identification of the compound

The pure product was obtained as a light yellowish needle-like crystal. After the compound was developed on the silica gel plates, purple spot and yellow stripe were presented using the ultraviolet spectrophotometer (365 nm) and the Iodine cylinder. Based on ^{13}C (100 MHz, DMSO-d_6) and ^{1}H (300 MHz, DMSO-d_6) NMR, the molecular formula of the compound was inferred as $C_{14}H_{13}NO_7$ and its unsaturation degree was determined as 9. Specifically, The ^{13}C NMR spectrum (100 MHz, DMSO-d_6) showed several carbon signals as follows: 152.4 (C-2), 144.8 (C-3), 133.5 (C-4), 132.2 (C-5), 129.3(C-6), 124.8 (C-7), 105.6 (C-8), 102.1 (C-9), 95.9 (C-10), 72.4 (C-11), 69.2 (C-12), 68.8 (C-13), 52.9 (C-14). According to the spectral data and comparison with published literature, the compound was identified as NCS, a Amaryllidaceae isocarbostyril alkaloid (Pettit and Melody, 2005). The chemical structure of NCS was demonstrated in supplementary material Fig. S2.

3.2. Cytotoxicity of NCS

The degrees of antiproliferation against L02, RAW264.7, MCF-7, Hep G2 and HT-29 cells after 72 treatment of NCS were investigated using MTT assay. The cell viability was expressed as the percentage of the cells in NCS-treated group compared with those in normal control group. At higher concentrations, NCS exhibited significant antiproliferative effects against Hep G2 and HT-29 (Fig. 1A) cells with the IC_{50} values of 0.08 μM and 1.373 μM, respectively. However, at lower concentrations, NCS did not inhibit but slightly promoted HT-29 and Hep G2 proliferation. These facts indicated that the concentration was very important for the anti-cancer efficacy of NCS. Unfortunately, considerable cytotoxicity of NCS on L02 (IC_{50} = 0.09 μM) and RAW264.7 (IC_{50} = 0.055 μM) cells was also intuitively observed.

Simultaneously, cell populations and morphological changes of L02 (Fig. 1C), Hep G2 (Fig. 1D), HT-29 (Fig. 1E) and RAW264.7 (Fig. 1F) cells after 72 h treatment of NCS were further illustrated. Obviously, great morphological changes were presented in the cancer cells as the cells lost their characteristic stretched appearance and shrinked to round, and showed clear cytoplasmic blebbing and vacuolation (Chen et al., 2016). Also, the cell populations decreased with the increasing concentrations of NCS.

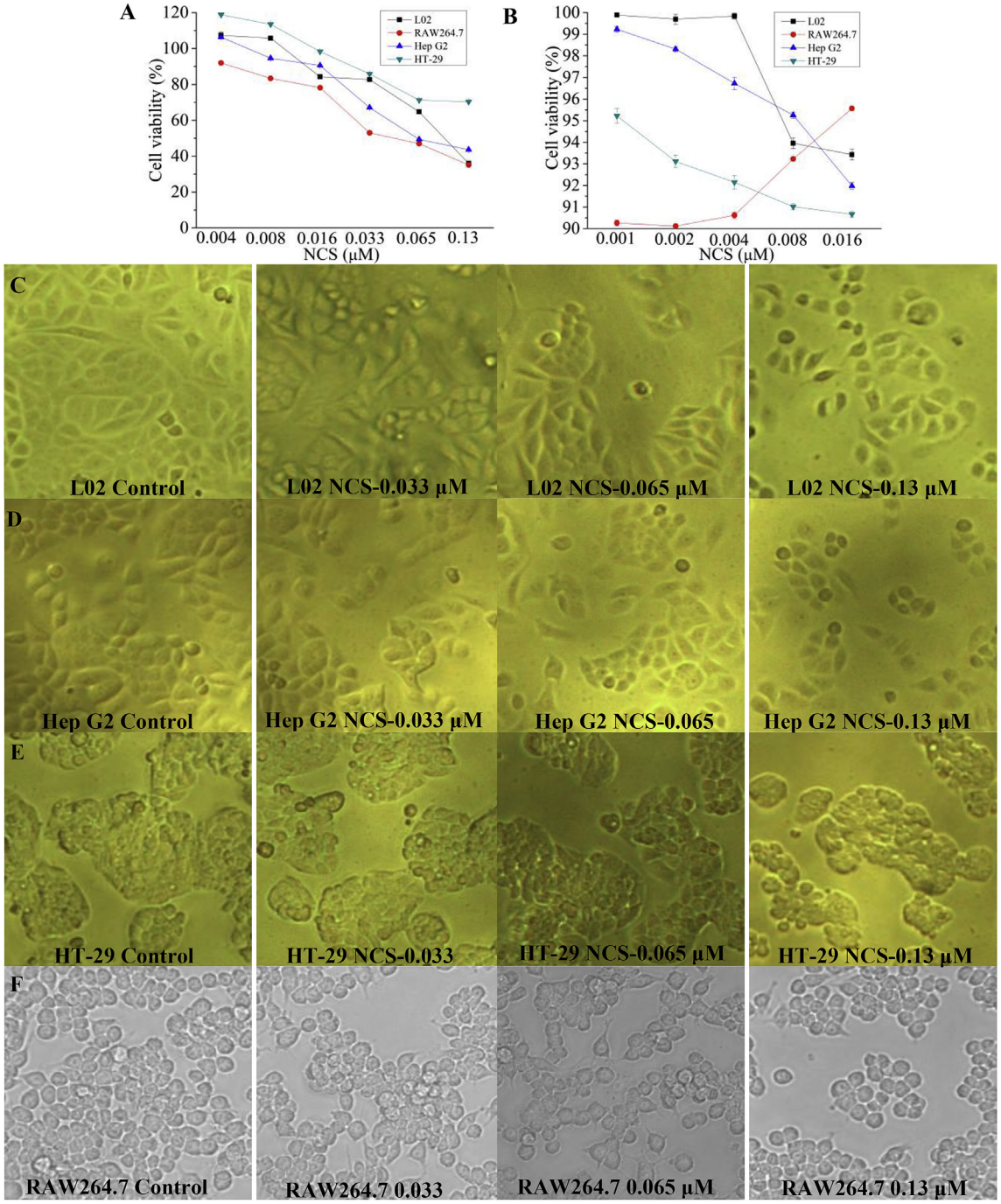

Fig. 1. Cell viability of L02, RAW264.7, Hep G2 and HT-29 after 72 h (A) and 24 h (B) treatment of NCS; Morphological illustrations of L02 (C), Hep G2 (D), HT-29 (E) and RAW264.7 (F) cell populations after 72 h treatment of NCS were also demonstrated. All images shown here were representative of three independent experiments with similar results.

3.3. Anti-inflammatory effect of NCS on RAW264.7 cells

3.3.1. Effect of NCS on LPS-induced production of NO and morphology in RAW264.7 cells

The cytotoxicity of NCS on L02, RAW264.7, Hep G2 and HT-29 cells at concentrations of 0.001, 0.002, 0.004, 0.008 and 0.016 μM for 24 h was evaluated and NCS did not alter cell viability of all the four cells (cell viability all exceeded 90%) (Fig. 1B). Therefore, 0.001–0.016 μM was screened as safe doses for NCS in further research. As shown in Fig. 2A, RAW264.7 cells displayed different morphological characteristics when stimulated with tested samples for 24 h. Briefly, cells in the control group showed round and regular shapes. However, pseudopodium occurred and the cells became bigger and irregular in shape when treated with LPS at 1 μg/mL. Luckily, this condition was improved after NCS (0.004, 0.008 and 0.016 μM) was added (Fig. 2A). Of note, NCS of the maximum concentration (0.016 μM) showed similar morphology with the positive control dexamethasone (DXM, 50 μg/mL). The results indicated that NCS displayed great anti-inflammatory potential even at low concentrations. NO production was also determined using Griess reagent and the data indicated that NCS at 0.004, 0.008 and 0.016 μM significantly inhibited NO accumulation in an intuitive dose dependent manner (Fig. 2B). Specifically, NCS at 0.008 and 0.016 μM showed greater inhibitory effects on NO production than DXM. In order to further explore the anti-inflammatory activity of NCS,

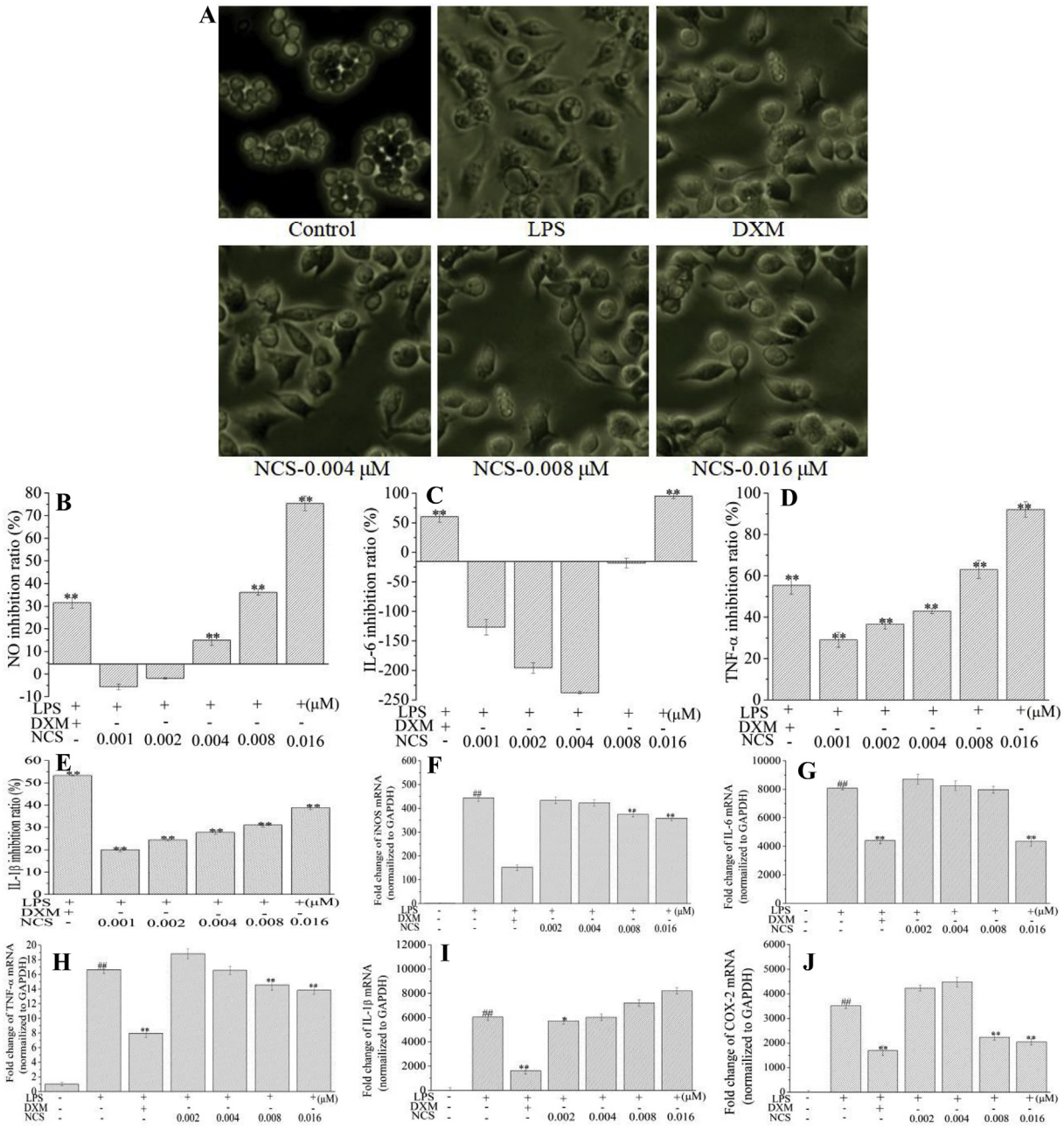

Fig. 2. Representative images of RAW264.7 cells under an inverted microscope after treated with NCS (A); effects of NCS on secretion of NO (B), IL-6 (C), TNF-α (D) and IL-1β (E); effects of NCS on expression of iNOS mRNA (F), IL-6 mRNA (G), TNF-α mRNA(H), IL-1β mRNA (I) and COX-2 mRNA (J). All experiments were run in triplicate, and data showed the mean ± SD values. (*) $p < 0.05$ and (**) $p < 0.01$ compared to the LPS-treated group.

ELISA, RT-qPCR and western blot analyses were performed in the following experiments.

3.3.2. Effect of NCS on LPS-induced production of IL-6, TNF-α and IL-1β

Stimulation with LPS resulted in a significant increase in the production of IL-6, TNF-α and IL-1β, as compared with the untreated control. However, these increases were potently suppressed by co-treatment with NCS. Briefly, NCS was a potent suppressant of IL-6 accumulation in the LPS-stimulated macrophages at 0.016 μM (Fig. 2C). Also, TNF-α production was also potently decreased in a dose-dependent manner after treated with NCS at various concentrations (Fig. 2D). Furthermore, NCS also dramatically and dose-dependently suppressed IL-1β production (Fig. 2E).

3.3.3. Effect of NCS on LPS-induced mRNA expression of iNOS, IL-6, TNF-α, IL-1β and COX-2

In order to examine whether NCS regulated pro-inflammatory cytokines and enzymes by inhibiting inflammation-associated genes, RT-qPCR analysis was conducted. High levels of iNOS, IL-6, TNF-α, IL-1β and COX-2 mRNAs were observed in the macrophages induced with LPS, and administration of NCS showed some certain inhibitory effects on the expression levels of these genes (Fig. 2F–J). NCS (0.008 and 0.016 μM) treatment significantly suppressed LPS-induced increases in mRNA expression levels of iNOS (Fig. 2F), TNF-α (Fig. 2H), COX-2 (Fig. 2J) at the transcriptional step, with a nearly maximum inhibitory effect at 0.016 μM. The elevated level of IL-6 mRNA in the LPS-induced RAW264.7 cells was also potently reduced by NCS (0.016 μM) treatment and the inhibitory activity was nearly comparable of DXM (Fig. 2G). Unexpectedly, NCS only showed slight inhibitory effects on

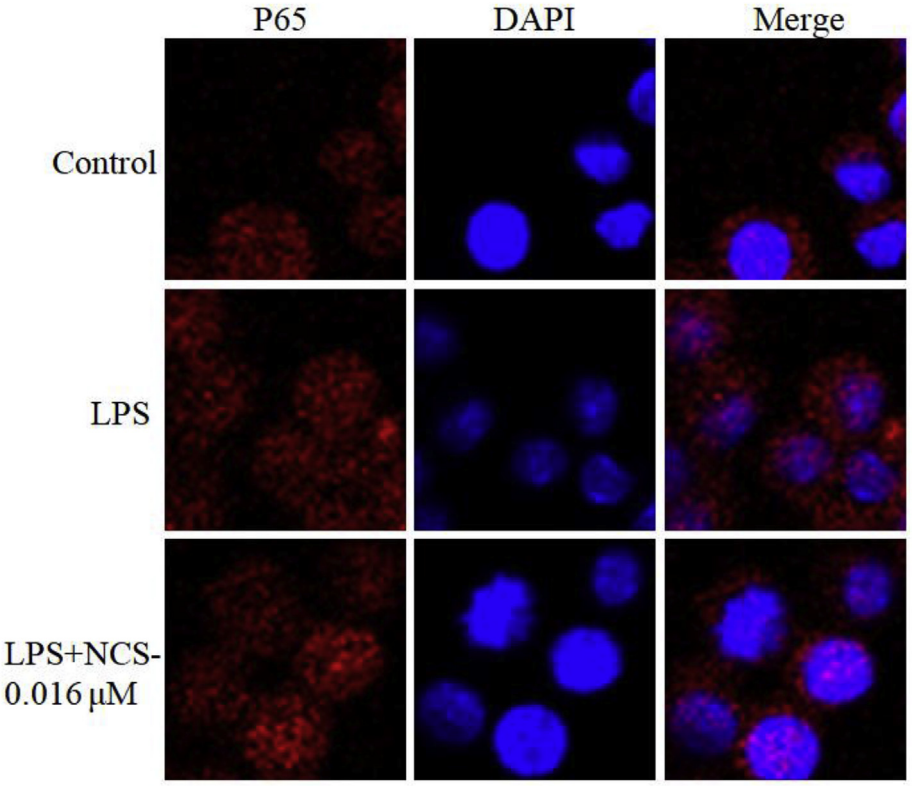

Fig. 3. Analysis of nuclear translocation of NF-κB determined by immunofluorescence analysis with laser scanning confocal microscope.

IL-1β mRNA expression at 0.002 μM, but instead up-regulated the expression level of IL-1β mRNA at 0.004, 0.008 and 0.016 μM (Fig. 2I). Collectively, these results indicated that NCS suppressed the secretion of NO, IL-6, TNF-α and IL-1β through inhibiting the expression of iNOS mRNA, IL-6 mRNA, TNF-α mRNA and IL-1β mRNA in LPS-stimulated mouse macrophages.

3.3.4. Effect of NCS on LPS-induced activation of NF-κB

As illustrated in Fig. 3, the signal intensity for P65 in the nuclei in LPS-induced cells was stronger than that in control cells, suggesting that NF-κB was activated by administration of LPS (1 μg/mL) and the cytosolic NF-κB subunit p65 significantly translocated to the nucleus. However, this event was suppressed by NCS (0.016 μM) treatment.

To further validated our results, western blot analysis was conducted. As shown in Fig. 4A-1, 1 μg/mL of LPS treatment resulted in more than 4-fold increase in phosphorylation of P65, and this increase was significantly inhibited by the addition of NCS at 0.008 and 0.016 μM. Furthermore, the nuclear translocation of NF-κB P65, phosphorylation and proteolytic degradation of IκBα, and the phosphorylation of IκKα/β, were all evaluated. As known, the P65 subunit was mostly present in the cytosol in un-treated normal cells. However, after administrated with LPS, the P65 subunit level in cytosol (Fig. 4B-1 and B-2) was dramatically down-regulated, and that in nuclear (Fig. 4C-1 and C-2) was significantly up-regulated in RAW264.7 cells. Luckily, these events were attenuated by the administration of NCS. The results suggested that NCS could inhibit the translocation of NF-κB subunit P65 from cytoplasm to nucleus. The conclusion was further confirmed by its suppressive effects on IκBα degradation and IκKα/β phosphorylation. Briefly, NCS dramatically decreased IκBα degradation (Fig. 4D-1 and D-2) and phosphorylation (Fig. 4E-1 and E-2), as well as the phosphorylation of IκKα/β (Fig. 4F-1 and F-2). Specifically, at 0.004 and 0.016 μM, NCS exhibited greater efficacy than that at 0.008 μM, suggesting that NCS did not inhibit IκBα degradation in a strict dose-dependent manner. Collectively, all these data indicated that NCS might inhibit inflammation-associated genes via regulation of the IκK-dependent canonical pathway of NF-κB activation.

3.3.5. Effect of NCS on LPS-induced phosphorylation of MAPKs

As shown in Fig. 5A, LPS treatment resulted in about a 2-fold increase in JNK phosphorylation, compared with normal control cells. Nevertheless, LPS-induced phosphorylation of JNK was significantly attenuated to 0.6036 and 0.6671 when LPS-induced macrophages were treated with NCS at concentrations of 0.004 and 0.016 μM, respectively. NCS supplementation (0.008 and 0.016 μM) also significantly blocked phosphorylation of P38 (Fig. 5B-1 and B-2).

3.3.6. Effect of NCS on LPS-induced activation of COX-2

As shown in Fig. 5C–-1 and C-2, NCS significantly inhibited COX-2 protein expression at 0.008 and 0.016 μM in a dose-dependent manner, consistent with its suppressive effect on COX-2 mRNA expression (Fig. 3I). In support, Liu et al. also extracted four new Amaryllidaceae alkaloids from *L. radiata* and found that (+)-1-hydroxy-ungeremine and (+)-N-methoxylcarbonyl-2-demethyl-isocorydione displayed anti-inflammation potential by selectively inhibiting COX-2 (Liu et al., 2015).

4. Discussion

Natural products have attracted intensive attention on discovering novel drugs for various human diseases (Jiang et al., 2007; Shen et al., 2017a). Especially, half of drugs with anti-tumor effects were natural origin (Altmann and Gertsch, 2007; Mann, 2002). Specifically, the promising activity of NCS has stimulated much effort toward its isolation and chemical characterization. NCS was firstly isolated from the bulbs of *Narcissus* species in 1967 (Ceriotti, 1967). Since then, NCS has been frequently reported to be isolated from the bulbs of *Narcissus* species (Weniger et al., 1995). In our current study, the content of NCS from *L. radiata* was 8.2 mg/kg, much higher than that of 4.16 mg/kg reported by Okamoto et al. (1968).

The most widely spread knowledge of NCS was its tremendous anti-

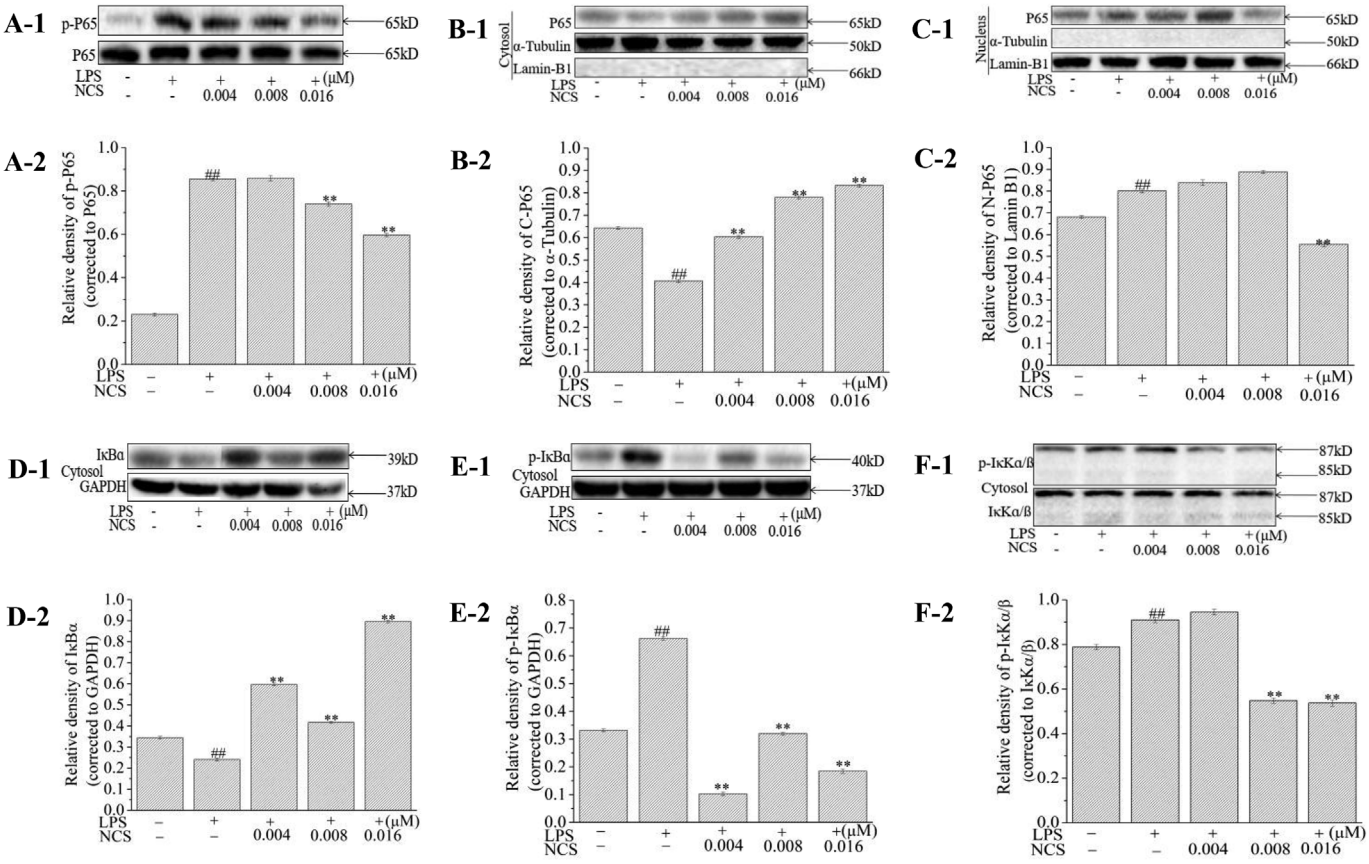

Fig. 4. Effects of NCS on phosphorylation of NF-κB P65 (A-1 and A-2), translocation of cytoplasmic NF-κB P65 (B-1 and B-2) and nuclear NF-κB P65 (C-1 and C-2), degradation (D-1 and D-2) and phosphorylation (E-1 and E-2) of cytoplasmic IκBα, phosphorylation of cytoplasmic p-IκKα/β (F-1 and F-2). α-Tubulin and Lamin B1were used as markers for cytoplasmic and nuclear proteins, respectively. All experiments were run in triplicate, and data showed the mean ± SD values. (*) $p < 0.05$ and (**) $p < 0.01$ compared to the LPS-treated group.

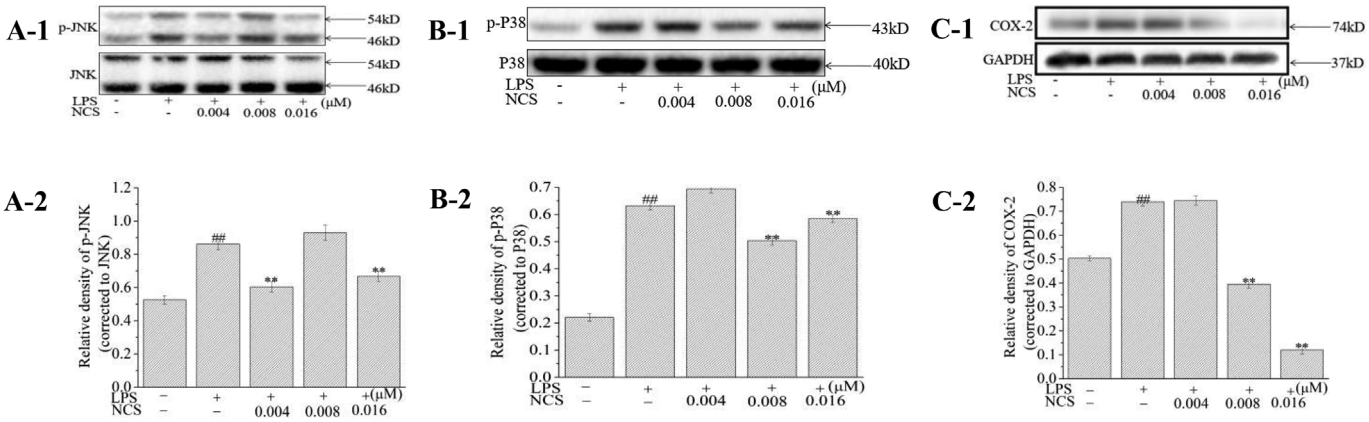

Fig. 5. Effects of NCS on phosphorylation of JNK (A-1 and A-2), phosphorylation of P38 (B-1 and B-2) and expression of COX-2 (C-1 and C-2). All experiments were run in triplicate, and data showed the mean ± SD values. (*) $p < 0.05$ and (**) $p < 0.01$ compared to the LPS-treated group.

cancer potential. Previous study *in vitro* frequently focused on the cytotoxicity of NCS on fibroblasts (IC_{50}: 7.5 μM) and cancer cells (IC_{50}: 30 nM), indicated that NCS was very sensitive to cancer cells and only higher concentrations of NCS could affect the viability of fibroblasts (Dumont et al., 2007). However, *in vivo* researches indicated that NCS only showed modest anti-tumor effects in mice with considerable toxicity (Van Goietsenoven et al., 2013). Thus, NCS has not been tested in human clinical trials up to now. The antiproliferation assay in this study revealed that NCS treatment for 72 h exhibited dose-dependently inhibitory effects against L02, RAW264.7, HT-29 and Hep G2 cells. The morphological changes further confirmed our results. The inhibitory effects on L02 and macrophages indicated that NCS might have significant side effects and therefore its application in clinical trials for cancer diseases must be prudent and further study was urgently needed.

There were published reports involving with the compound responsible for the anti-cancer activity of *L. radiata*. For example, Chen et al. screened out hippeastrine from *L. radiata* by combining affinity ultrafiltration with topoisomerase I as a target enzyme, and they found that hippeastrine might be the specific alkaloid which was responsible for the anti-cancer activity of crude Amaryllidaceae alkaloids isolated

from *L. radiata* (Chen et al., 2016). They demonstrated that hippeastrine exhibited marked antiproliferative properties against Hep G2 cells (IC_{50}: 11.85 ± 0.20 μg/mL) and HT-29 (IC_{50}: 3.98 ± 0.29 μg/mL) cells. Of note, the IC_{50} values of NCS on Hep G2 and HT-29 cells were much lower that of hippeastrine, indicating that NCS might also be a specific alkaloid responsible for the cytotoxicity of *L. radiata*. Further study is still on-going in our laboratory.

Many products have been found to exert inhibitory effects on pro-inflammatory cytokines via MAPK and NF-κB signaling pathways (Bi et al., 2016; Cheng et al., 2008; Ko et al., 2016; Seong et al., 2016). Published reports proved that MAPK phosphorylation could induce NF-κB activation (Guha and Mackman, 2001; Nakano et al., 1998). Seong et al. reported that methanol extracts from *Gnaphalium affine* exerted anti-inflammatory effects through suppressing MAPK and NF-κB signaling pathways in LPS-induced RAW264.7 cells (Seong et al., 2016). Also, alternaramide, isolated from the extract of the marine-derived fungus *Alternaria* sp. SF-5016, also significantly inhibited JNK and P38 phosphorylation in LPS-induced RAW264.7 and BV2 cells (Liao et al., 2016).

It was reported that IL-6, TNF-α and IL-1β genes were closely dependent on the activation of NF-κB pathway (Arend and Dayer, 1995; Koch, 2005). The secretion of TNF-α and IL-1β could inhibit the mRNA expression of iNOS at the transcriptional level, thus down-regulating NO production (Lee et al., 2008). Our data strongly demonstrated that NCS probably exerted anti-inflammatory effects through inhibiting activation of NF-κB and phosphorylation of MAPK, thereby suppressing the production of NO, IL-6, TNF-α and IL-1β. Consistent with our experimental data, published reports also demonstrated that NCS could suppress TNF-α secretion in LPS-stimulated RAW264.7 cells (Yamazaki and Kawano, 2011; Yui et al., 2001).

Taken together, these results suggested that NCS might be a very promising anti-inflammatory candidate for the therapy of inflammation-associated diseases at even very low concentrations. Future study should focus on the possible antiproliferative and anti-inflammatory molecular mechanisms induced by NCS, and this is going on in our laboratory.

Acknowledgements

This project was supported by Science and Technology Project of Guangzhou City (201604020150).

Appendix A. Supplementary data

Supplementary data to this article can be found online at https://doi.org/10.1016/j.fct.2019.02.003.

Transparency document

Transparency document related to this article can be found online at https://doi.org/10.1016/j.fct.2019.02.003.

References

Altmann, K.H., Gertsch, J., 2007. Anticancer drugs from nature - natural products as a unique source of new microtubule-stabilizing agents. Nat. Prod. Rep. 24, 327–357. https://doi.org/10.1039/b515619j.

Arend, W.P., Dayer, J.M., 1995. Inhibition of the production and effects of interleukin-1 and tumor necrosis factor alpha in rheumatoid arthritis. Arthritis Rheum. 38, 151–160. https://doi.org/10.1002/art.1780380202.

Bender, O., Gunduz, M., Cigdem, S., Hatipoglu, O.F., Acar, M., Kaya, M., Grenman, R., Gunduz, E., Ugur, K.S., 2018. Functional analysis of ESM1 by siRNA knockdown in primary and metastatic head and neck cancer cells. J. Oral Pathol. Med. 47, 40–47. https://doi.org/10.1111/jop.12648.

Bi, C.L., Wang, H., Wang, Y.J., Sun, J., Dong, J.S., Meng, X., Li, J.J., 2016. Selenium inhibits Staphylococcus aureus-induced inflammation by suppressing the activation of the NF-kappa KB and MAPK signalling pathways in RAW264.7 macrophages. Eur. J. Pharmacol. 780, 159–165. https://doi.org/10.1016/j.ejphar.2016.03.044.

Bustin, S.A., Vandesompele, J., Pfaffl, M.W., 2009. Standardization of qPCR and RT-qPCR. Genetic Engineering & Biotechnology News 29, 40–43.

Caivano, M., 1998. Role of MAP kinase cascades in inducing arginine transporters and nitric oxide synthetase in RAW264 macrophages. FEBS Lett. 429, 249–253. https://doi.org/10.1016/S0014-5793(98)00578-X.

Ceriotti, G., 1967. Narciclasine: an antimitotic substance from Narcissus bulbs. Nature 213, 595–596. https://doi.org/10.1038/213595a0.

Chen, G.L., Tian, Y.Q., Wu, J.L., Li, N., Guo, M.Q., 2016. Antiproliferative activities of Amaryllidaceae alkaloids from Lycoris radiata targeting DNA topoisomerase I. Sci. Rep. 6. https://doi.org/10.1038/srep38284.

Cheng, Y.W., Chang, C.Y., Lin, K.L., Hu, C.M., Lin, C.H., Kang, J.J., 2008. Shikonin derivatives inhibited LPS-induced NOS in RAW 264.7 cells via downregulation of MAPK/NF-kappa B signaling. J. Ethnopharmacol. 120, 264–271. https://doi.org/10.1016/j.jep.2008.09.002.

Dumont, P., Ingrassia, L., Rouzeau, S., Ribaucour, F., Thomas, S., Roland, I., Darro, F., Lefranc, F., Kiss, R., 2007. The amaryllidaceae isocarbostyril narciclasine induces apoptosis by activation of the death receptor and/or mitochondrial pathways in cancer cells but not in normal fibroblasts. Neoplasia 9, 766–776. https://doi.org/10.1593/neo.07535.

Guha, M., Mackman, N., 2001. LPS induction of gene expression in human monocytes. Cell. Signal. 13, 85–94. https://doi.org/10.1016/S0898-6568(00)00149-2.

He, M., Qu, C., Gao, O., Hu, X., Hong, X., 2015. Biological and pharmacological activities of amaryllidaceae alkaloids. RSC Adv. 5, 16562–16574. https://doi.org/10.1039/c4ra14666b.

Hu, F., Yang, S., Zhao, D., Zhu, S., Wang, Y., Li, J., 2012. Moderate extracellular acidification inhibits capsaicin-induced cell death through regulating calcium mobilization, NF-kappa B translocation and ROS production in synoviocytes. Biochem. Biophys. Res. Commun. 424, 196–200. https://doi.org/10.1016/j.bbrc.2012.06.115.

Jiang, J.G., Huang, X.J., Chen, J., Lin, Q.S., 2007. Comparison of the sedative and hypnotic effects of flavonoids, saponins, and polysaccharides extracted from Semen Ziziphus jujube. Nat. Prod. Res. 21, 310–320. https://doi.org/10.1080/14786410701192827.

Kang, J., Zhang, Y., Cao, X., Fan, J., Li, G., Wang, Q., Diao, Y., Zhao, Z., Luo, L., Yin, Z., 2012. Lycorine inhibits lipopolysaccharide-induced iNOS and COX-2 up-regulation in RAW264.7 cells through suppressing P38 and STATs activation and increases the survival rate of mice after LPS challenge. Int. Immunopharm. 12, 249–256. https://doi.org/10.1016/j.intimp.2011.11.018.

Ko, W., Sohn, J.H., Jang, J.H., Ahn, J.S., Kang, D.G., Lee, H.S., Kim, J.S., Kim, Y.C., Oh, H., 2016. Inhibitory effects of alternaramide on inflammatory mediator expression through TLR4-MyD88-mediated inhibition of NF-kappa B and MAPK pathway signaling in lipopolysaccharide-stimulated RAW264.7 and BV2 cells. Chem. Biol. Interact. 244, 16–26. https://doi.org/10.1016/j.cbi.2015.11.024.

Koch, A.E., 2005. Chemokines and their receptors in rheumatoid arthritis future targets? Arthritis Rheum. 52, 710–721. https://doi.org/10.1002/art.20932.

Lee, S.J., Nam, W.D., Na, H.J., Cho, Y.L., Ha, K.S., Hwang, J.Y., Lee, H., Kim, S.O., Kwon, Y.G., Kim, Y.M., 2008. CT20126, a novel immunosuppressant, prevents collagen-induced arthritis through the down-regulation of inflammatory gene expression by inhibiting NF-kappa B activation. Biochem. Pharmacol. 76, 79–90. https://doi.org/10.1016/j.bcp.2008.04.006.

Li, C.Y., Wang, Y., Wang, H.L., Shi, Z., An, N., Liu, Y.X., Liu, Y., Zhang, J., Bao, J.K., Deng, S.P., 2013. Molecular mechanisms of Lycoris aurea agglutinin-induced apoptosis and G2/M cell cycle arrest in human lung adenocarcinoma A549 cells, both in vitro and in vivo. Cell Prolif 46, 272–282. https://doi.org/10.1111/cpr.12034.

Liao, C., Zheng, K., Li, Y., Xu, H., Kang, Q., Fan, L., Hu, X., Jin, Z., Zeng, Y., Kong, X., Zhang, J., Wu, X., Wu, H., Liu, L., Xiao, X., Wang, Y., He, Z., 2016. Gypenoside L inhibits autophagic flux and induces cell death in human esophageal cancer cells through endoplasm reticulum stress-mediated Ca2+ release. Oncotarget 7, 47387–47402. https://doi.org/10.18632/oncotarget.10159.

Liu, Z.M., Huang, X.Y., Cui, M.R., Zhang, X.D., Chen, Z., Yang, B.S., Zhao, X.K., 2015. Amaryllidaceae alkaloids from the bulbs of Lycoris radiata with cytotoxic and anti-inflammatory activities. Fitoterapia 101, 188–193. https://doi.org/10.1016/j.fitote.2015.01.003.

Lubahn, C., Schaller, J.A., Shewmacker, E., Wood, C., Bellinger, D.L., Byron, D., Melody, N., Pettit, G.R., Lorton, D., 2012. Preclinical efficacy of sodium narcistatin to reduce inflammation and joint destruction in rats with adjuvant-induced arthritis. Rheumatol. Int. 32, 3751–3760. https://doi.org/10.1007/s00296-011-2217-z.

Mann, J., 2002. Natural products in cancer chemotherapy: past, present and future. Nat. Rev. Canc. 2, 143–148. https://doi.org/10.1038/nrc723.

Mikami, M., Kitahara, M., Kitano, M., Ariki, Y., Mimaki, Y., Sashida, Y., Yamazaki, M., Yui, S., 1999. Suppressive activity of lycoricidinol (narciclasine) against cytotoxicity of neutrophil-derived calprotectin, and its suppressive effect on rat adjuvant arthritis model. Biol. Pharm. Bull. 22, 674–678.

Nakano, H., Shindo, M., Sakon, S., Nishinaka, S., Mihara, M., Yagita, H., Okumura, K., 1998. Differential regulation of I kappa B kinase alpha and beta by two upstream kinases, NF-kappa B-inducing kinase and mitogen-activated protein kinase ERK kinase kinase-1. Proc. Natl. Acad. Sci. U. S. A. 95, 3537–3542. https://doi.org/10.1073/pnas.95.7.3537.

Okamoto, T., Torii, Y., Isogai, Y., 1968. Lycoricidinol and lycoricidine, new plant-growth regulators in the bulbs of Lycoris radiata herb. Chem. Pharmaceut. Bull. 16, 1860–1864.

Pettit, G.R., Melody, N., 2005. Antineoplastic agents. 527. Synthesis of 7-deoxynarcistatin, 7-deoxy-trans-dihydronarcistatin, and trans-dihydronarcistatin 1. J. Nat. Prod. 68, 207–211. https://doi.org/10.1021/np0304518.

Pettit, G.R., Melody, N., Herald, D.L., 2001. Antineoplastic agents. 450. Synthesis of (+)-pancratistatin from (+)-narciclasine as relay. J. Org. Chem. 66, 2583–2587.

Sener, B., Orhan, I., Satayavivad, J., 2003. Antimalarial activity screening of some alkaloids and the plant extracts from Amaryllidaceae. Phytother Res. 17, 1220–1223.

https://doi.org/10.1002/ptr.1346.
Seong, Y.A., Hwang, D., Kim, G.D., 2016. The anti-inflammatory effect of Gnaphalium affine through inhibition of NF-kappa B and MAPK in lipopolysaccharide-stimulated RAW264.7 cells and analysis of its phytochemical components. Cell Biochem. Biophys. 74, 407–417. https://doi.org/10.1007/s12013-016-0744-7.
Shen, C.Y., Jiang, J.G., Yang, L., Wang, D.W., Zhu, W., 2017a. Anti-ageing active ingredients from herbs and nutraceuticals used in traditional Chinese medicine: pharmacological mechanisms and implications for drug discovery. Br. J. Pharmacol. 174, 1395–1425. https://doi.org/10.1111/bph.13631.
Shen, C.Y., Yang, L., Jiang, J.G., Zheng, C.Y., Zhu, W., 2017b. Immune enhancement effects and extraction optimization of polysaccharides from Citrus aurantium L. var. amara Engl. Food & Function 8, 796–807. https://doi.org/10.1039/c6fo01545j.
Shen, C.Y., Zhang, W.L., Jiang, J.G., 2017c. Immune-enhancing activity of polysaccharides from Hibiscus sabdariffa Linn. via MAPK and NF-kappa B signaling pathways in RAW264.7 cells. Journal of Functional Foods 34, 118–129. https://doi.org/10.1016/j.jff.2017.03.060.
Van Goietsenoven, G., Andolfi, A., Lallemand, B., Cimmino, A., Lamoral-Theys, D., Gras, T., Abou-Donia, A., Dubois, J., Lefranc, F., Mathieu, V., Kornienko, A., Kiss, R., Evidente, A., 2010. Amaryllidaceae alkaloids belonging to different structural subgroups display activity against apoptosis-resistant cancer cells. J. Nat. Prod. 73, 1223–1227. https://doi.org/10.1021/np9008255.
Van Goietsenoven, G., Mathieu, V., Lefranc, F., Kornienko, A., Evidente, A., Kiss, R., 2013. Narciclasine as well as other amaryllidaceae isocarbostyrils are promising GTP-ase targeting agents against brain cancers. Med. Res. Rev. 33, 439–455. https://doi.org/10.1002/med.21253.
Vanden Berghe, W., Plaisance, S., Boone, E., De Bosscher, K., Schmitz, M.L., Fiers, W., Haegeman, G., 1998. p38 and extracellular signal-regulated kinase mitogen-activated protein kinase pathways are required for nuclear factor kappa B p65 transactivation mediated by tumor necrosis factor. J. Biol. Chem. 273, 3285–3290. https://doi.org/10.1074/jbc.273.6.3285.
Weniger, B., Italiano, L., Beck, J.P., Bastida, J., Bergonon, S., Codina, C., Lobstein, A., Anton, R., 1995. Cytotoxic activity of Amaryllidaceae alkaloids. Planta Med. 61, 77–79.
Yamazaki, Y., Kawano, Y., 2011. Inhibitory effects of herbal alkaloids on the tumor necrosis factor-alpha and nitric oxide production in lipopolysaccharide-stimulated RAW264 macrophages. Chem. Pharmaceut. Bull. 59, 388–391. https://doi.org/10.1055/s-2006-958007.
Yui, S., Mikami, M., Mimaki, Y., Sashida, Y., Yamazaki, M., 2001. Inhibition effect of Amaryllidaceae alkaloids, lycorine and lycoricidinol on macrophage TNF-alpha production. Yakugaku Zasshi-Journal of the Pharmaceutical Society of Japan 121, 167–171. https://doi.org/10.1248/yakushi.121.167.